Incorporating Linear Synchronous Transit Interpolation into the Growing String Method: Algorithm and Applications

Andrew Behn,[†] Paul M. Zimmerman,[‡] Alexis T. Bell,[†] and Martin Head-Gordon[*,‡]

[†]Department of Chemical and Biomolecular Engineering and [‡]Department of Chemistry, University of California, Berkeley, California 94720-1462, United States

ABSTRACT: The growing string method is a powerful tool in the systematic study of chemical reactions with theoretical methods which allows for the rapid identification of transition states connecting known reactant and product structures. However, the efficiency of this method is heavily influenced by the choice of interpolation scheme when adding new nodes to the string during optimization. In particular, the use of Cartesian coordinates with cubic spline interpolation often produces guess structures which are far from the final reaction path and require many optimization steps (and thus many energy and gradient calculations) to yield a reasonable final structure. In this paper, we present a new method for interpolating and reparameterizing nodes within the growing string method using the linear synchronous transit method of Halgren and Lipscomb. When applied to the alanine dipeptide rearrangement and a simplified cationic alkyl ring condensation reaction, a significant speedup in terms of computational cost is achieved (30–50%).

■ INTRODUCTION

One of the key contributions of theoretical chemistry to the systematic study of chemical reactions is the ability to accurately predict kinetic rate constants. These kinetic rate constants are typically calculated with transition state theory, which requires knowledge of the transition state structure. While locating stable minima on the potential energy surface (PES) is considered relatively easy in theoretical chemistry, the automated location of first order transition states remains a challenge.

The principle method for obtaining exact first order transition states connecting known reactant and product configurations is to first generate a rough guess of the structure and then refine this structure to the exact answer through surface walking.[1−4] The algorithms for surface walking are similar to the algorithms which locate PES minima. Because there are many more transition states than minima on a typical PES, this guess must be very close (within the basin of attraction) to the proper transition state in order to properly converge. Once the transition state has been refined, it must be confirmed by integrating the reaction path downhill to the reactant and product configurations.[5,6]

Several algorithms for finding transition state guesses from known reactant and product configurations have been developed,[7−33] including the nudged elastic band method (NEB),[5−8] the string method (SM),[11−16] and the growing string method (GSM).[17−22] In each of these "chain-of-states" methods,[23] the minimum energy pathway is located by iteratively optimizing a discretized representation of the pathway. Each of the nodes in the chain-of-states is a full molecular structure at some intermediate stage of the transition between the reactant and product. Optimization steps are taken by moving each image downhill on the PES, perpendicular to the direction of the reaction path. Additionally, the nodes in the chain are kept equally spaced through the optimization process, either through an additional spacing force or by explicit reparameterization. This ensures that this node-based description of the pathway does not contain large gaps, where the PES may be left unsampled.

When using *ab initio* surfaces in each of these methods, the overall cost of generating a suitable guess of the transition state can be stated in terms of the overall number of QM nuclear gradient calculations performed. All other calculations needed to perform these methods can be considered negligible. Higher order derivatives of the QM energy, such as the nuclear Hessian, would provide faster convergence but are typically expensive in *ab initio* calculations.

The most commonly encountered chain-of-states method is the nudged elastic band method,[7,8] which finds an approximate reaction path by optimizing a series of images connected to each other through a set of springs with contrived hooke constants. The optimization step direction for each node, v_{NEB}^i, is comprised of two components, as shown in eq 1.

$$\hat{v}_{NEB}^i = \frac{-g_i^{\perp} + f_i^{\parallel}}{|-g_i^{\perp} + f_i^{\parallel}|} \tag{1}$$

The first term is the perpendicular force, used to minimize the energy of each node, and is given by eq 2.

$$-g_i^{\perp} = -(I - \hat{t}_i \hat{t}_i^T)g_i \tag{2}$$

The tangent direction, $\hat{t}_i$, is typically found by normal finite difference, but other schemes have been proposed for improved performance.[9,10] The second term, $f_i^{\parallel}$, expanded in eq 3, is a force along the reaction path which arises from the springs that connect each node in the chain to its neighbors. Here, k is the spring constant, and R denotes the coordinates of a molecular structure.

$$f_i^{\parallel} = \hat{t}_i \hat{t}_i^T [(R_{i+1} - R_i) - (R_i - R_{i-1})]k \tag{3}$$

This component is added to ensure that the images remain equally spaced during the optimization process.

A slightly newer method, similar in concept to the nudged elastic band, is the string method.[11−16] The reaction path is again represented by a series of molecular images, but optimization is broken into two separate steps: evolution and reparameterization. In the evolution step, the molecular images are moved in the direction of the negative perpendicular gradient, similarly to the first term in eq 1. The tangent direction is determined by creating a cubic spline through each Cartesian coordinate of the string of images. The reparameterization step is performed by reinterpolating the molecular images along this set of cubic splines to achieve the desired parametrization density. This avoids the need to decide an arbitrary spring constant, as in the NEB.

The growing string method[17−22] is a modification of the original string method that aims to reduce overall computational cost by "growing" the set of nodes from the reactant and product configurations inward toward the transition state. In principle, this avoids performing gradient calculations on excessively rugged parts of the PES that are far from the final reaction pathway. Initially, the string consists of only the reactant and product configurations, with one node being added to each side during the first reparameterization. The string is then evolved and reparameterized in the normal fashion until the specified convergence criteria for node addition are achieved by the innermost nodes on the reactant and product sides. New nodes are added accordingly until the string is fully populated. The string then continues to optimize until convergence is reached. Several schemes have been developed to accelerate practical use by improving optimization, and using cost-saving dual basis techniques.[18−20]

The nudged elastic band and string method both require initial pathways from which the optimizations are launched. This initial pathway has a tremendous impact on convergence and must be chosen carefully.[14] Cartesian interpolation may work for some simple reactions; however, it is not always an appropriate choice. Reactions such as the HNC to HCN isomerization are poorly described by Cartesian interpolation despite having only a handful of internal degrees of freedom. Such simple reactions, as well as more complex reactions with many atoms, require an interpolation scheme with the chemical intuition built-in. GSM does not require a full initial guess pathway but does require a methodology for reparameterizing and interpolating new nodes.

To alleviate this shortcoming of GSM specifically (and more generally the SM and NEB), we propose using linear synchronous transit (LST) interpolation[34,35] for node interpolation and reparameterization. LST is a method for interpolating between two fixed molecular geometries that seeks to preserve internuclear distances within the molecule as it morphed from one to the other. In doing so, the usual drawbacks of Cartesian interpolation in which chemical bonds are overly compressed or stretched are avoided. A simple example of the contrast between LST and Cartesian interpolation is demonstrated in Figure 1 with the HCN to HNC isomerization. In this paper, we demonstrate the advantages of LST interpolation in GSM by direct comparison to Cartesian interpolation.

■ MODIFIED IMPLEMENTATION OF THE GROWING STRING METHOD

I. Evolution Step. To demonstrate the use of LST versus Cartesian interpolation within the GSM, a modified version of the algorithm was developed. The evolution step is performed by moving each current node in the string, i, along the negative
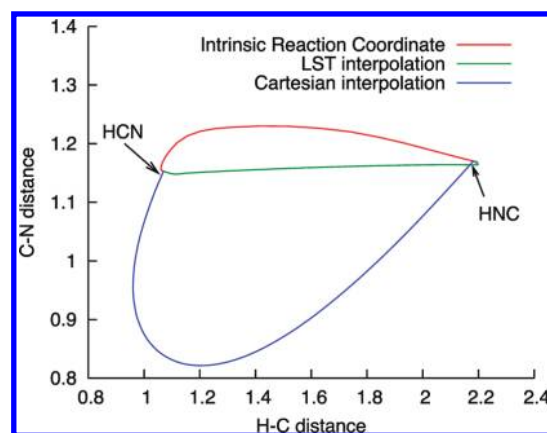

Figure 1. Contrast of Cartesian and LST interpolation between reactant and product configurations of the HCN to HNC reaction. Note that the Cartesian interpolated pathway is far from the minimum energy path, while the LST interpolated pathway is rather close. In addition, the LST method's tendency to preserve internuclear distances is clearly shown.

perpendicular gradient, as shown in eq 4. The tangent direction is determined for each node with either LST interpolation or by computing the cubic splines over the set of Cartesian coordinates of the string.

$$\hat{v}_i = \frac{-(I - t_i t_i^T) g_i}{|(I - t_i t_i^T) g_i|} = \frac{-g_i^\perp}{|g_i^\perp|} \tag{4}$$

The length of each node's evolution step is computed by dividing the magnitude of the node's perpendicular gradient by a common scaling factor, γ, as shown in eq 5. This produces a damped steepest descent step and has the effect of generating a large step when there is a large perpendicular gradient far from convergence and a small step when the node is near convergence.

$$d_i = \frac{|g_i^\perp|}{\gamma} \tag{5}$$

The overall step, Δx_i, as a combination of eqs 4 and 5 is presented in eq 6.

$$\Delta x_i = \hat{v}_i d_i = \frac{-g_i^\perp}{\gamma} \tag{6}$$

This step differs from the original GSM,[17] which seeks to minimize the string by taking several small trial steps in the downhill direction, fitting the observed energy profile to a quadratic function, and moving to the estimated minimum.

II. Reparameterization Step. After each evolution step, the string is reparameterized to achieve a uniform node density along the arclength of the reaction path. If nodes are numbered starting with the reactant node as $i = 1$ and the product node as $i = N$, where N is the number of nodes in the fully populated string, the desired parametrization is given by eq 7. N_R and N_P are the number of nodes on the reactant and product sides respectively, and s_{tot} is the current total arclength from reactant to product. The exact computation of s_{tot} is done with the appropriate interpolation scheme (discussed below).

$$s_i = s_{tot}\left(\frac{i-1}{N-1}\right) \quad \text{for } i \leq N_R \text{ and } N - N_P < i \leq N \tag{7}$$
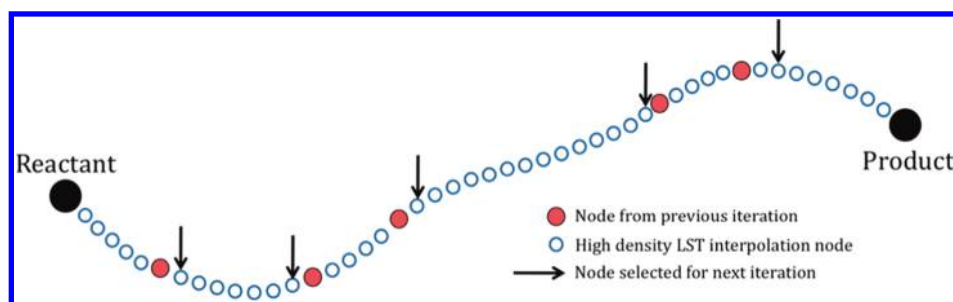
Figure 2. Cartoon of the strategy for using LST interpolation within the GSM. The spaces between the previous iteration nodes are filled with a discrete set of LST interpolated images. The set of interpolated images which returns the appropriate parameterization density is then returned for the next iteration.

The algorithm is started with two nodes on each side of the string—the fixed reactant and product structures and one variable node on each side. Once the magnitude of the perpendicular gradient for the innermost node for a side has fallen below the specified tolerance for node addition, a new node is added to a side by incrementing N_R or N_P during the reparameterization step. This has the effect of growing a new node on the appropriate side until the string is fully populated. Once the full string has been grown, convergence may be considered. The objective function for locating the minimum energy path (MEP) is the sum of the perpendicular gradient magnitudes for each node, as indicated by eq 8. If the end points are assumed to be stable minima on the PES, they may be neglected in the sum since they contribute nothing.

$$F = \sum_{i=2}^{N-1} |g_i^{\perp}| \qquad (8)$$

■ INTERPOLATION METHOD

If Cartesian coordinates with cubic splines are used for reparameterization, the procedure is straightforward. A cubic spline is determined for each Cartesian coordinate using the structures of the nodes and their positions along the string in terms of arclength, and the appropriate nodes are interpolated.

The use of linear synchronous transit reparameterization is slightly more complicated. It is based on the use of LST interpolation between two fixed molecular images, as given by the resultant structure in the minimization of eq 9.

$$G = \sum_{a>b}^{atoms} \frac{(r_{ab}^i - r_{ab}^c)^2}{(r_{ab}^i)^4} + 10^{-6} \sum_{a=1}^{atoms} \sum_{j=x,y,z} (w_{a,j}^i - w_{a,j}^c)^2 \qquad (9)$$

The r variables denote internuclear distances, while the w variables denote pure Cartesian coordinates. The i and c superscripts denote "interpolated" versus "computed" values respectively. The interpolated values are determined by mixing the values of the fixed molecular structures, while the computed values are derived from the interpolated structure being optimized to minimize G. We are careful to stress that the "computed" internuclear distances, r_{ab}^c, are derived from the coordinates provided by the Cartesian "computed" structure, w^c. Thus, there is only one full set of Cartesian coordinates being manipulated. The numerator of the first term of eq 9 serves to preserve internuclear distances from being overly stretched or compressed during interpolation, while the denominator weights

this effect in favor of shorter internuclear distances (i.e., bonding interactions). The second term of eq 9 provides a small force to align the interpolated molecule with the fixed end structures.

Equation 9 fails to adequately show that the "interpolated" values must be computed by choosing a mixing ratio, f, of the two fixed structures. This is shown in eq 10, where the superscripts 1 and 2 denote the fixed end point structures.

$$\begin{aligned} r_{ab}^i &= r_{ab}^1 + f(r_{ab}^2 - r_{ab}^1) \\ w_{a,j}^i &= w_{a,j}^1 + f(w_{a,j}^2 - w_{a,j}^1) \end{aligned} \qquad (10)$$

From these equations, it becomes obvious that G is really $G = G(f)$, and the choice of f (between 0 and 1) will determine how close the interpolated image is to the fixed end points. A value of $f = 0$ will produce an interpolated structure identical to structure 1, while $f = 1$ will reproduce structure 2. If all values of f between 0 and 1 are sampled and the LST equation minimized at each value, it yields a continuous description of the deformation from structure 1 to structure 2, with an integrated arclength of s_{LST} (f). There exists a monotonically increasing but nonlinear mapping between f and $s_{LST}(f)$ such that it is impossible to know *a priori* which value of f to use to return a desired value of s_{LST}. To avoid this problem, a high-density series of LST interpolations must be performed between each neighboring set of nodes in the evolving string.

The general strategy for using LST interpolation for reparameterization in GSM is shown in Figure 2. First, a high-density set of LST interpolations is performed between each neighboring pair of nodes. From this, the normalized arclength position of each interpolated node along the growing string is computed. Finally, the nodes which yield the appropriate node spacing, as given by eq 7, are selected from the high-density string and taken as the reparameterized string. From this same high density LST interpolated string, the tangent vector at each selected node is computed and stored.

■ COMPUTATIONAL DETAILS

The examples detailed below demonstrate the use of Cartesian and LST interpolation in our modified implementation of the growing string method interfaced with Q-Chem 3.2.[36] For each example, a string of 11 nodes was grown from the reactant and product structures and optimized until a specified objective function was achieved. At the beginning of the GSM execution, the reactant and product structures were aligned to be in maximum coincidence in non mass-weighted Cartesian coordinates.[37] This step is essential to ensure that the rotational and translational degrees of freedom between the two structures
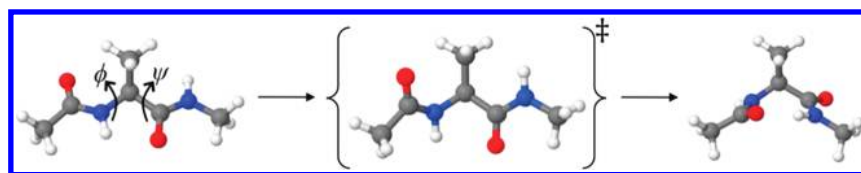
Figure 3. The reactant, transition state, and product configurations for the alanine–dipeptide rearrangement reaction.

Table 1. Dihedral Angles (in degrees) of the Alanine Dipeptide Isomerization

	ϕ	ψ
C_5	−161.5	167.1
TS	113.7	−141.9
C_{7AX}	72.5	−59.5

do not significantly affect the interpolation. It also ensures that the computed arclength between nodes does not include appreciable noninternal motion.

The scaling factor used to generate the step length of each node during the evolution step was $\gamma = 5.0$ hartree/Å^2. Reparameterization was performed after each evolution step, with new nodes added to the string (during the reparameterization steps) if the magnitude of the perpendicular gradient at a frontier node fell below 0.1 hartree/Å. For reparameterization and node addition with LST, 200 images were included in each high-density interpolation string running from reactant to product. The structures of this high-density string were optimized with Newton–Rasphon minimization of eq 9 to a tolerance of $|\nabla G| <$ 0.001 when computed in units of Ångstroms.

After the string was fully optimized, the nodes of the string were used as the starting point of a surface walking transition state optimization calculation in Q-Chem. This algorithm, which operates in delocalized internal coordinates, seeks to maximize the energy along the eigenvector of the lowest Hessian eigenmode and minimize the energy along all other eigenmodes. To aid in these calculations, an exact Hessian was calculated at the outset of the search and updated via the Powell/Murtagh–Sargent scheme.[38,39]

Once a first-order saddle point was isolated from these optimizations, a high-quality MEP was integrated downhill from the transition state, via the Schlegel–Gonzalez MEP following algorithm[6] in non-mass-weighted Cartesian coordinates, to ensure that the transition state connected the reactant and product structures initially fed to the growing string method. It is possible that multiple transition states may be found if each node is used to launch a calculation. For elementary reaction steps, only the highest energy node for an adequately converged string should result in a meaningful transition state. For nonelementary reaction steps, legitimate transition states may be found for each elementary reaction. Both of these possibilities are explored in the test cases presented below.

■ ALANINE DIPEPTIDE REARRANGEMENT

A common test problem for the benchmarking of MEP and transition state finding algorithms is the rearrangement of alanine dipeptide from the C_5 isomer to the C_{7AX} isomer. The minimum energy pathway involves the concerted rotation of the two dihedral angles, ϕ and ψ, shown in Figure 3. The relevant values of the dihedral angles for the reactant, TS, and product in the gas
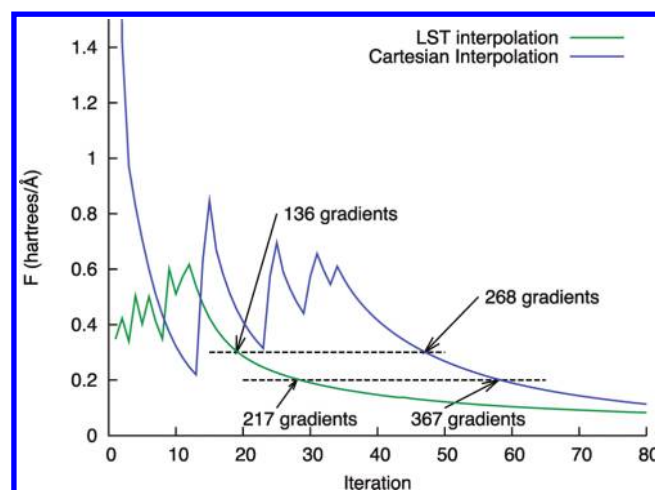

Figure 4. Objective fuction, F, vs iteration for the alanine dipeptide rearrangement reaction. The spikes in the initial portion of each curve indicate the addition of new nodes during the growth phase.

phase at the B3LYP/6-31G level of theory given in the work of Perczel et al.[40] are shown in Table 1. This is the same level of theory used in the present example.

Figure 4 shows the value of the objective function F (from eq 8) as a function of iteration. These curves can each be broken into two regions: growth and refinement. The initial growth phase, during which new nodes are still being added to the string, results in the spikes seen initially in Figure 4. Since the number of nodes in each iteration is not constant in this phase, the number of QM gradients necessary for each iteration also varies. The subsequent refinement phase begins once the string has been fully grown and is marked by the monotonically decreasing value of F during which the string settles into the reaction pathway. For alanine dipeptide rearrangement with Cartesian interpolation, the growth phase is completed after the 33rd iteration, corresponding to 133 QM gradient calculations. With LST interpolation, growth is completed after the 11th iteration and 55 QM gradient calculations (see Figure 5 for a comparison of the intermediate energy profiles for the LST and Cartesian GSM). The growth phase is much faster with LST due to the superior quality of the new interpolated nodes. This demonstrated in Figure 6, which shows the energy as a function of iteration for the first node added to the reactant side of the string. The LST interpolated node begins at a much lower energy and achieves the threshold for the next node addition more quickly.

Table 2 lists the number of QM gradient calculations necessary to fully grow the string and achieve the desired level of convergence. For a convergence criterion of 0.3 hartree/Å, LST interpolation reduces the number of QM gradients required by 49%, effectively doubling the speed of GSM. The string energy profiles for each interpolation method at a convergence of $F = 0.3$
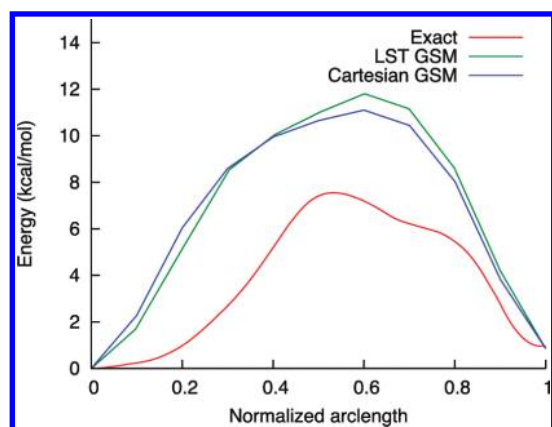
Figure 5. Comparison of the intermediate energy profiles for the LST and Cartesian GSM and the exact MEP energy profile for the alanine dipeptide rearrangement. The GSM energy profiles are snapshots taken when the objective function, F, reached 0.3 hartree/Å.
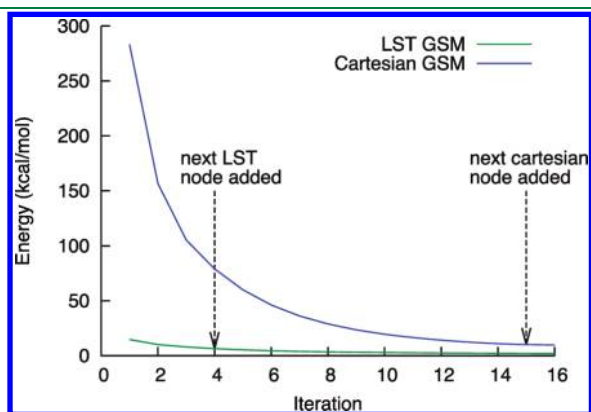

Figure 6. Energy of the first interior node from the reactant side versus iteration for the alanine dipeptide rearrangement. Note that the LST interpolated node begins at a much lower energy than the Cartesian interpolated node and achieves the threshold for node addition much sooner.

Table 2. Computational Cost in QM Gradients for the Alanine Dipeptide Rearrangement, with Speedup for LST versus Cartesian Interpolation

conv. criteria	method	QM gradients	speedup
0.3 hartree/Å	Cartesian	268	49%
	LST	136	
0.2 hartree/Å	Cartesian	367	41%
	LST	217	

hartree/Å shown in Figure 6 indicate that the overall quality of the string with Cartesian and LST interpolation is approximately the same. For a more tightly converged reaction coordinate at F = 0.2 hartree/Å, the speedup is similar at 41%. For each of the four strings resulting from LST and Cartesian interpolation methods in GSM at these two convergence criteria, the highest energy node yields the proper transition state using the standard Q-Chem surface-walking algorithm detailed in the Computational Details section.

■ RING CONDENSATION REACTION

The second benchmarking case is the cationic ring condensation of 2-(but-3-enyl)oxiranium to 4-hydroxycyclohexan-1-ylium. This reaction is inspired by the much more complicated (and enzymatically catalyzed) reaction of 2,3-oxidosqualene to produce lanosterol during cholesterol synthesis.[41] Even though this reaction is simplified, it possesses four transition states on the path from linear reactant to final product at the gas-phase HF/STO-3 g level of theory. Each of these transition states and the stable intermediates are depicted in Figure 7. TS1, TS2, and TS4 are each internal rotations of the molecule with small barriers between 2.0 and 3.0 kcal/mol. The remaining transition state, TS3, involves the rearrangement of bond orders and possesses a much higher barrier of 23.2 kcal/mol.

Figure 8 shows the convergence rate of GSM with both Cartesian and LST interpolation for this reaction. With Cartesian interpolation, the growth phase is completed after 36 iterations, which corresponds to 186 QM gradient calculations. With LST interpolation, the growth phase requires only 16 iterations,
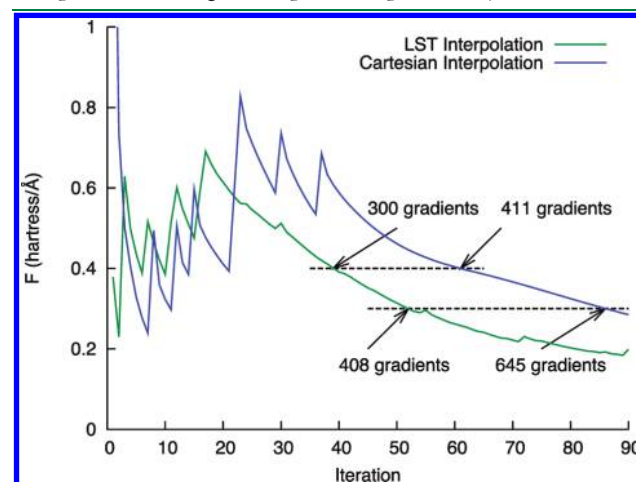

Figure 8. Objective fuction, F, versus iteration for the cationic ring condensation reaction. The spikes in the initial portion of each curve indicate the addition of nodes during the growth phase.
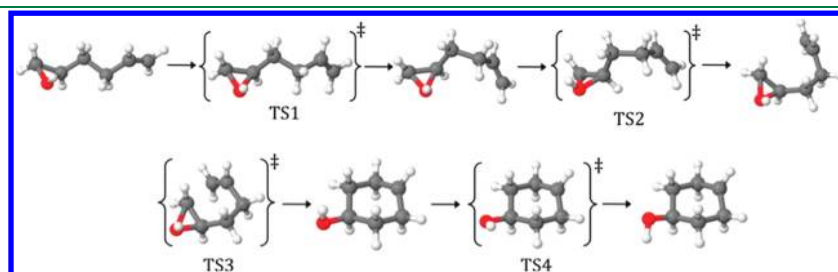

Figure 7. Reactant, product, stable intermediates, and transition states on the pathway between the linear and ring structures.

Table 3. Computational Costs, Speedups, and Success in Identifying Various TS Structures for the Cationic Ring Condensation Reaction

conv. criteria	method	QM gradients	speedup	TS1	TS2	TS3	TS4
0.4 hartree/Å	Cartesian	411	27%	Y	Y	Y	N
	LST	300		Y	Y	Y	N
0.3 hartree/Å	Cartesian	645	37%	Y	Y	Y	N
	LST	408		Y	Y	Y	Y
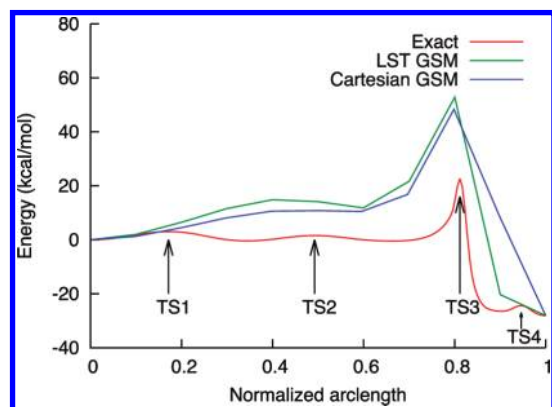
Figure 9. Comparison of the intermediate energy profiles for the LST and Cartesian GSM and the exact MEP energy profile for the ring condensation reaction. The GSM energy profiles are snapshots taken when the objective function, F, reached 0.3 hartree/Å.

corresponding to 84 QM gradient calculations. As denoted in Table 3, a 27% reduction in the number of gradients is observed for convergence to $F = 0.4$ hartree/Å, and a 37% reduction is observed for convergence to $F = 0.3$ hartree/Å. Figure 9 shows the exact energy profile for this reaction, as well as the energy profiles for both GSM executions once the objective function reached 0.3 hartree/Å.

In each of the four cases noted in Table 3, launching TS optimization calculations in Q-Chem[36] from the converged strings' nodes resulted in several first order transition states. In all cases, TS1, TS2, and TS3 from Figure 7 were successfully recovered. However, TS4 (which involves a subtle hydroxyl group rotation) was only observed for the more tightly converged ($F = 0.3$ hartree/Å) LST interpolated string.

■ CONCLUSIONS

The growing string method is a powerful tool in the study of chemical reactions from an *ab initio* perspective because it allows for the rapid identification of transition states, from which approximate kinetic rate constants may be computed with transition state theory. However, the interpolation method by which the string is reparameterized and new nodes are added during the growth phase has a large impact on the rate of convergence and thus the quality of results. In particular, choosing an interpolation scheme which compresses or expands chemical bonds arbitrarily can necessitate a large number of QM calculations in order to properly find the minimum energy path and transition state.

Our results indicate that using the linear synchronous transit method developed initially by Halgren and Lipscomb[34] can be a powerful addition to the traditional growing string method. This

interpolation method is an improvement over Cartesian interpolation because it preserves bond lengths and performs rotational rearrangements seamlessly. The guessed pathways are thus closer to the final result and require less computational effort to optimize.

When applied to the isomerization of alanine dipeptide, GSM with LST interpolation requires roughly half of the computational effort as GSM with Cartesian interpolation. In the condensation of 2-(but-3-enyl)oxiranium to 4-hydroxycyclohexan-1-ylium, computational cost is reduced by roughly one-third when LST interpolation is used. In this latter reaction, which contains multiple transition states between the reactant and product, the LST version of the GSM proves superior by properly identifying every transition state (major and minor) where the Cartesian version misses at least one.

■ AUTHOR INFORMATION

Corresponding Author
*E-mail: mhg@cchem.berkeley.edu.

Notes

The authors declare no competing financial interest.

■ ACKNOWLEDGMENT

■ REFERENCES

(1) Cerjan, C. J.; Miller, W. H. *J. Chem. Phys.* **1981**, *112*, 2129.
(2) Banerjee, A.; Adams, N.; Simons, J.; Shepard, R. *J. Phys. Chem.* **1985**, *89*, 52.
(3) Hrantchian, H. P.; Schlegel, H. B. *J. Comput. Chem.* **2003**, *24*, 1514.
(4) Schlegel, H. B. *J. Comput. Chem.* **2003**, *24*, 1514.
(5) Fukui, K. *J. Phys. Chem.* **1970**, *74*, 4161.
(6) Gonzalez, C.; Schlegel, H. B. *J. Chem. Phys.* **1989**, *90*, 2154.
(7) Mills, G.; Jonsson, H. *Phys. Rev. Let* **1994**, *72*, 1124.
(8) Henkelman, G.; Jonsson, H. *J. Chem. Phys.* **2000**, *113*, 9978.
(9) Henkelman, G.; Uberuaga, B. P.; Jonsson, H. *J. Chem. Phys.* **2000**, *113*, 9901.
(10) Trygubenko, S. A.; Wales, D. J. *J. Chem. Phys.* **2004**, *120*, 2083.
(11) E, W.; Ren, W.; Vanden-Eijnden, E. *Phys. Rev. B.* **2002**, *66*, 052301.
(12) E, W.; Ren, W.; Vanden-Eijnden, E. *J. Phys. Chem. B.* **2005**, *109*, 6688.
(13) E, W.; Ren, W.; Vanden-Eijnden, E. *J. Chem. Phys.* **2007**, *126*, 164103.
(14) Sheppard, D.; Terrell, R.; Henkelman, G. *J. Chem. Phys.* **2008**, *128*, 134106.
(15) Burger, S. K.; Yang, W. *J. Chem. Phys.* **2006**, *124*, 054109.
(16) Burger, S. K.; Yang, W. *J. Chem. Phys.* **2007**, *127*, 164107.
(17) Peters, B.; Heyden, A.; Bell, A. T. *J. Chem. Phys.* **2004**, *120*, 7877.
(18) Goodrow, A.; Bell, A. T.; Head-Gordon, M. *J. Chem. Phys.* **2008**, *129*, 174109.
(19) Goodrow, A.; Bell, A. T.; Head-Gordon, M. *J. Chem. Phys.* **2009**, *130*, 244108.
(20) Goodrow, A.; Bell, A. T.; Head-Gordon, M. *Chem. Phys. Lett.* **2010**, *484*, 393.
(21) Quapp, W. *J. Comput. Chem.* **2007**, *28*, 1834.
(22) Quapp, W. *J. Theor. Comput. Chem.* **2009**, *8*, 101.
(23) Elber, R.; Karplus, M. *Chem. Phys. Lett.* **1987**, *139*, 375.

(24) Ayala, P. Y.; Schlegel, H. B. *J. Chem. Phys.* **1997**, *107*, 375.

(25) del Campo, J. M.; Koster, A. M. *J. Chem. Phys.* **2008**, *129*, 024107.

(26) Ghasemi, S. A.; Goedecker, S. *J. Chem. Phys.* **2011**, *135*, 014108.

(27) Burger, S. K.; Ayers, P. W. *J. Chem. Phys.* **2010**, *132*, 234110.

(28) Maeda, S.; Morokuma, K. *J. Chem. Phys.* **2010**, *132*, 241102.

(29) Dey, B. K.; Ayers, P. W. *Mol. Phys.* **2006**, *104*, 541.

(30) Aguilar-Mogas, A.; Gimenez, X.; Bofill, J. M. *J. Chem. Phys.* **2008**, *128*, 104102.

(31) Aguilar-Mogas, A.; Gimenez, X.; Bofill, J. M. *J. Comput. Chem.* **2010**, *31*, 2510.

(32) Klimes, J.; Bowler, D. R.; Michaelides, A. *J. Phys: Condens. Mater.* **2010**, *22*, 074203.

(33) Koslover, E. F.; Wales, D. J. *J. Chem. Phys.* **2007**, *127*, 134102.

(34) Halgren, T. A.; Lipscomb, W. N. *Chem. Phys. Lett.* **1977**, *49*, 225.

(35) Peng, C.; Schlegel, H. B. *Israel J. Chem* **1993**, *33*, 449.

(36) Shao, Y.; et al. *Phys. Chem. Chem. Phys.* **2006**, *8*, 3172.

(37) Rhee, Y. M. *J. Chem. Phys.* **2000**, *113*, 6021.

(38) Powell, M. J. D. *Math. Prog.* **1971**, *1*, 26.

(39) Murtagh, B. A.; Sargent, R. W. H. *Comput. J.* **1972**, *13*, 185.

(40) Perczel, A.; Farkas, O.; Jakli, I.; Topol, I. A.; Csizmadia, I. G. *J. Comput. Chem.* **2002**, *24*, 1026.

(41) Wendt, K. U.; Schulz, G. E.; Corey, E. J.; Liu, D. R. *Angew. Chem., Int. Ed.* **2000**, *39*, 2812.

4025

dx.doi.org/10.1021/ct200654u |*J. Chem. Theory Comput.* 2011, 7, 4019–4025